Heliyon

ELSEVIER

Received:
26 January 2019
Revised:
7 March 2019
Accepted:
2 April 2019

Cite as: Ghulam Rasool, Ting Zhang. Characteristics of chemical reaction and convective boundary conditions in Powell-Eyring nanofluid flow along a radiative Riga plate. Heliyon 5 (2019) e01479. doi: 10.1016/j.heliyon.2019.e01479

Characteristics of chemical reaction and convective boundary conditions in Powell-Eyring nanofluid flow along a radiative Riga plate

Ghulam Rasool *, **Ting Zhang**

School of Mathematical Sciences, Zhejiang University, Hangzhou 310027, PR China

* Corresponding author.
E-mail address: grasool@zju.edu.cn (G. Rasool).

Abstract

A typical base fluid such as water, oil or glycol is poor conductor of heat due to deficient thermo-physical properties. This deficiency is normally addressed by saturation of thermally strong conductive metallic nanoparticles such as Fe, Ti, Hg, Cu, Au into the base fluid resulting a stronger thermal conductivity, electric conductivity, heat and mass flux of the so formulated nanofluid. Nanoparticles having a diameter size less than 100 nano-meter are preferred in this formulation because these nano-sized particles stay suspended into the base fluid for a longer time-period. This communication aims to investigate the salient features of a nanofluid flow along a radiative Riga plate using Powell-Eyring model and convective boundary conditions. The flow model involves the effect of first order chemical reaction as well as the Brownian motion diffusion and Thermophoresis effects. Governing PDEs are transformed into ODEs using suitable transformations. HAM is applied for convergent series solutions to the boundary value problem. Impact of various parameters including Brownian motion, Thermophoresis, modified Hartman number, Lewis and Prandtl number on flow profiles is analyzed graphically. Parameters of physical interest like Skin-friction, Nusselt and Sherwood numbers are illustrated through numerical data. Effect of modified Hartman number is significant

https://doi.org/10.1016/j.heliyon.2019.e01479

on flow profiles due to involvement of Riga plate. An efficiency is achieved in fluid flow and heat-mass flux through suspension of nanoparticles in base fluid.

Keywords: Applied mathematics, Condensed matter physics, Electromagnetism, Thermodynamics

1. Introduction

Recent studies have revealed that high profile cooling is mandatory for most of the technological as well as industrial processes. This high efficiency in heat-mass flux is not easy to achieve with typical fluids having poor thermo-physical properties. The issue was addressed to some extent by the introduction of the concept of nanofluids. A nanofluid is a fluid saturated with highly conductive nano-size metallic particles. These nanoparticles easily stay suspended in the base fluid for sufficiently longer time-period as compared to larger particles. Named after the great work presented by Choi [1] and the subsequent literature, nanofluids are remarkably promising in heat and mass transfer applications especially in micro processing, heat exchangers, aerospace technology, automotives and refrigeration etc. where high level energy devices are involved with a very small size and squeezed shape. Nanofluids are equally important for medical point of view. For example, the treatment of cancer by therapy, hyperthermia, treatment of wounds, surgeries and opening/unblocking the arteries etc. are direly dependent on the applications of nanofluids. Buongiorno [2] applied the idea of nanofluid and developed a mathematical model to explore and analyze the thermal characteristics of base fluids. The model is comprised of two factors, the Brownian motion factor (Nb) and the thermophoresis factor (Nt). Later on, numerous developments have been made in the field of nanofluids that can be seen in reference cited in this text (see [3, 4, 5, 6, 7, 8, 9, 10, 11, 12, 13, 14, 15, 16, 17, 18, 19, 20, 21]) and cross references cited therein.

In fluid mechanics the importance of magnetic field holds a key place due to its various applications in enhancement of thermo-physical characteristics of a fluid. Fields such as astrology and earth sciences encounter many fluids that are poor conductors of electricity. Thus, an external agent is always needed to enhance the heat transfer phenomena through better conductivity and other related thermo-physical properties. This external agent could be a magnetic bar or permanently fixed array of such magnets with alternating electrodes. This kind of formulation was first done in Riga by Gailitis and Lielausis [22] and was given the name of Riga plate. The so formulated Riga plate is so convenient that it took no time to get famous in industrial processes involving fluid flow phenomena. Ahmed et al. [23] studied the impact of heating with zero mass flux at the surface. The conduction was eased by using a Riga plate in the model to involve the effect of Lorentz force that decays exponentially with increasing displacement from the surface of

plate. Sheikholeslami et al. [24] studied the impact of Lorentz forces on Marangoni convection of nanofluid. Shafiq et al. [25] studied fluid point flow based on Walters-B model through Riga plate. Adeel et al. [26] analyzed mixed convection of nanofluids with vertically placed Riga plate in the fluid flow. Recently, Rasool et al. [27] reported the impact of thermal radiation on Marangoni convective nanofluid flow towards a Riga plate.

Complicated systems in fluid mechanics undergo various chemical reactions inside the fluid. These reactions are of various types such as homogeneous reactions, heterogeneous reactions etc. having significant impact on the flow profiles. Chaudhary and Merkin [28] presented the impact of chemical reactions on a stagnation point fluid flow utilizing (i) equal and (ii) different diffusivities for auto-catalyst and reactants. Merkin [29] analyzed viscous flow alongside a flat plate considering the effect of reactions. Merkin et al. [30] is an extension of Merkin [29] to interpret the loss of catalyst. Khan and Pop [31, 32] investigated the effect of chemical reactions on viscoelastic fluids. The viscoelastic parameter reduced significantly for the presented model.

Complex rheological fluids are always difficult to be predicted through Navier stokes equations. Grease, human blood, various paints, typical oil and polymer solutions etc. are typical examples of such fluids. There is a highly non-linear relation between stress and strain in such type of fluids as compared to the Newtonian fluids. To analyze their behavior, various models have been proposed including the Powell-Eyring model that is under consideration in this study. At an extreme shear stress rate, the fluid behaves like a Newtonian fluid however, it behaves like a non-Newtonian fluid at an intermediate shear stress rate. Instead of empirical relation, the extrapolation of constitutive expressions from kinetic theory of gases is a significant characteristic of this model. The model is important for its various industrial applications especially in polymer and chemical engineering processes. Numerous researches have been carried out in the context of Powell-Eyring nanofluid and its engineering and industrial application (see [33, 34, 35, 36, 37, 38] and reference cited therein).

The inspiration for this work is covered by three main aspects. Firstly, to formulate an incompressible nanofluid flow along a radiative Riga-plate in the presence of first order chemical reaction and convective boundary conditions at the surface. There is no literature available on such formulation in the past. Secondly, to interpret the effect of Thermophoresis, Brownian motion and Lorentz force generated by Riga plate on the velocity, temperature and concentration profiles. Finally, to note the variation in skin friction (wall drag force), Nusselt and Sherwood number that are significantly important factors in industrial applications of nanofluids.

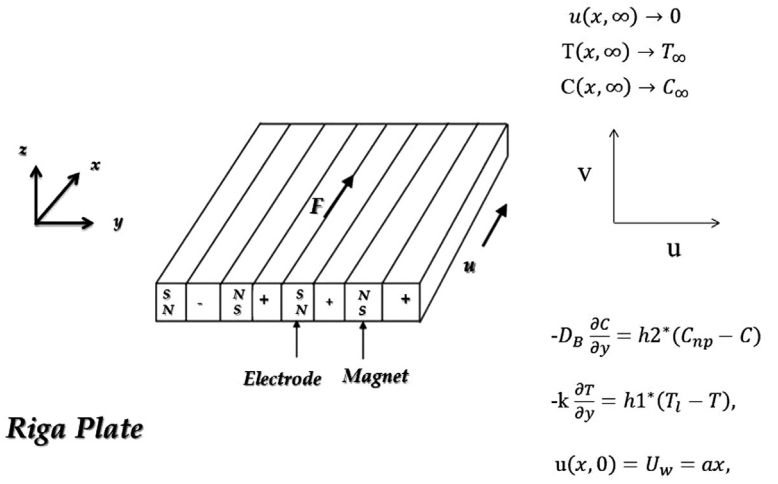

Figure 1. Schematic diagram.

2. Model

We assume an incompressible steady Powell-Eyring nanofluid flow along a radiative Riga surface in two-dimensions. Convective boundary conditions for heat and mass are utilized. The surface of Riga plate is heated because of hot fluid having initial temperature T_l with concentration of nanoparticles C_{np}, respectively that gives rise to h_1^* and h_2^*, the heat and mass transport coefficients. The fluid behaves electrically conducting along y-axis due to the Lorentz force generated by Riga plate as well as the nanoparticles saturation into the base fluid. The Lorentz force incorporated in the model using Grinberg term decays exponentially with an increasing displacement from the surface of plate. The x-axis is taken along the surface of Riga plate. The y-axis is taken normal to it. Schematic diagram can be seen in Figure 1. Following Hayat et al. [39] together with the Grinberg term and the first order chemical reaction term, the boundary value problem has following governing PDEs with subsequent BCs,

$$\frac{\partial u}{\partial x} + \frac{\partial v}{\partial y} = 0, \tag{1}$$

$$u\frac{\partial u}{\partial x} + v\frac{\partial u}{\partial y} = \left(\nu + \frac{1}{\rho_l \gamma C^*}\right)\frac{\partial^2 u}{\partial y^2} - \frac{1}{2\rho_l \gamma C^{*3}}\left(\frac{\partial u}{\partial y}\right)^2 \frac{\partial^2 u}{\partial y^2} + \left(\frac{\pi . j_0 . M_0 \exp(\frac{-\pi y}{b})}{8\rho_l}\right), \tag{2}$$

$$u\frac{\partial T}{\partial x} + v\frac{\partial T}{\partial y} = \alpha\frac{\partial^2 T}{\partial y^2} + \tau\left(D_B\frac{\partial T}{\partial y}\frac{\partial C}{\partial y} + \frac{D_T}{T_\infty}\left(\frac{\partial T}{\partial y}\right)^2\right) - \frac{1}{(\rho c)_l}\frac{\partial q_r}{\partial y}, \tag{3}$$

$$u\frac{\partial C}{\partial x} + v\frac{\partial C}{\partial y} = D_B\left(\frac{\partial^2 C}{\partial y^2}\right) + \frac{D_T}{T_\infty}\left(\frac{\partial^2 T}{\partial y^2}\right) - K(C - C_\infty), \tag{4}$$

such that,

$$u = xa, \quad v = 0, \quad -k\frac{\partial T}{\partial y} = h_1^*(T_l - T), \quad -D_B\frac{\partial C}{\partial y} = h_2^*(C_{np} - C) \qquad \text{at } y = 0,$$
$$u \to 0, \quad T \to T_\infty, \quad C \to C_\infty \quad \text{as } y \to \infty, \tag{5}$$

where μ represents dynamic viscosity, ρ_l is used for density of base fluid, ν represents kinematic viscosity, γ and C^* denote the material constants, σ represents the electric-conductivity, α is the thermal diffusivity, k is called thermal conductivity of nanofluid, $(\rho c)_l$ is called the heat capacity of nanofluid, D_B is used for Brownian diffusion, D_T is used for thermophoretic diffusion, T_∞ and C_∞ are the temperature and concentration distributions away from Riga surface. j_0 is the density of applied current through electrodes, M_0 is the magnetization in magnets, b is width of magnets and electrodes and τ is the ratio between productive heat capacity of fluid and nanoparticles. q_r represents the radiative heat-flux. Using Rosseland's approximation and Taylor series expansion with omission of higher order terms beyond the 1st degree, we have,

$$T^4 \cong T_\infty^3(4T - 3T_\infty). \tag{6}$$

Eq. (6) in Eq. (7) yields,

$$\frac{\partial q_r}{\partial y} = -\frac{16\sigma^* T_\infty^3}{3k^*}\frac{\partial^2 T}{\partial y^2}. \tag{7}$$

Using (7) in (3), we have,

$$u\frac{\partial T}{\partial x} + v\frac{\partial T}{\partial y} = \alpha\frac{\partial^2 T}{\partial y^2} + \frac{(\rho c)_p}{(\rho c)_l}\left(D_B\left(\frac{\partial T}{\partial y}\frac{\partial C}{\partial y}\right) + \frac{D_T}{T_\infty}\left(\frac{\partial T}{\partial y}\right)^2\right) + \frac{16\sigma^* T_\infty^3}{3k^*(\rho c)_l}\frac{\partial^2 T}{\partial y^2}. \tag{8}$$

Define,

$$u = \frac{\partial \psi}{\partial y}, \quad v = -\frac{\partial \psi}{\partial x},$$
$$\sqrt{\frac{\nu}{a}}\eta = y, \quad \frac{\psi}{x\sqrt{\nu a}} = f(\eta), \tag{9}$$
$$\theta(\eta) = \frac{T - T_\infty}{T_l - T_\infty}, \quad \phi(\eta) = \frac{C - C_\infty}{C_{np} - C_\infty}.$$

System (9) in equations (1), (2), (3) and (4), results in following nonlinear ODEs with subsequent boundary conditions,

$$f''' + Kf''' - K\Lambda f''^2 f''' + ff'' - f'^2 + Q\exp(-\beta\eta) = 0, \tag{10}$$
$$\left(1 + \frac{4}{3}Rd\right)\theta'' + \Pr\left(Nb\theta'\phi' + f\theta' + Nt\theta'^2\right) = 0, \tag{11}$$
$$\phi'' + Le\Pr\left(f\phi' - K_1\phi\right) + \frac{Nt}{Nb}\theta'' = 0, \tag{12}$$

$$f = 0, \quad \frac{\partial f}{\partial \eta} = 1, \quad \frac{\partial \theta}{\partial \eta} = -\alpha_1(1-\theta(0)), \quad \frac{\partial \phi}{\partial \eta} = -\alpha_2(1-\phi(0)) \text{ at } \eta = 0, \tag{13}$$

$$\frac{\partial f}{\partial \eta} \to 0, \ \theta \to 0, \ \phi \to 0 \text{ as } \eta \to \infty. \tag{14}$$

Here Pr represent the Prandtl factor, Q is used for modified Hartman number, β is known as dimensionless parameter, Rd is the symbol of radiation parameter, Nb is the Brownian motion, Nt is the Thermophoretic parameter, Λ and K are fluid parameters, Le is Lewis number, α_1 and α_2 are heat-mass transfer Biot factors and K_1 represents the chemical reaction, respectively. Mathematically,

$$\begin{aligned} &\mathrm{Pr} = \frac{\nu}{\alpha}, \quad Q = \frac{\pi j_0 M_0}{8\rho_l x a^2}, \quad \beta = \frac{\pi}{b}\sqrt{\frac{\nu}{a}}, \quad Rd = \frac{4\sigma^* T_\infty^3}{kk^*}, \\ &Nb = \frac{(\rho c)_p D_B (C_{np} - C_\infty)}{(\rho c)_l \nu}, \quad Nt = \frac{(\rho c)_p D_T \left(T_l - T_\infty\right)}{(\rho c)_l \nu T_\infty}, \quad \Lambda = \frac{u^3}{2\nu x C^{*2}}, \\ &K = \frac{1}{\mu\gamma C^*}, \quad Le = \frac{\alpha}{D_B}, \quad \alpha_1 = \frac{h_1^*}{k}\sqrt{\frac{\nu}{a}}, \quad \alpha_2 = \frac{h_2^*}{D_B}\sqrt{\frac{\nu}{a}}. \end{aligned} \tag{15}$$

Skin-friction (drag force), Nusselt number (heat flux) and Sherwood number (mass flux) are written below,

$$\begin{aligned} &Re_x^{1/2} C_{fx} = \left((1+K)f''(0) - \frac{1}{3}K\Lambda f''^3(0)\right), \\ &Re_x^{-1/2} Nu_x = -\left(1 + \frac{4}{3}Rd\right)\theta'(0), \\ &Re_x^{-1/2} Sh_x = -\phi'(0), \end{aligned} \tag{16}$$

where Re_x represents the local Reynolds.

3. Methodology

Homotopy analysis method (HAM) is independent of small as well as large physical parameters. Thus, it is more efficient as compared to perturbation technique and other conventional methods for solving nonlinear systems. It is applicable in most of nonlinear system of equations developed in science problems, engineering and finance without small or large parameters [40, 41, 42, 43, 44, 45]. For convergent series solutions through HAM, we assume,

$$f_0 = 1 - e^{-\eta}, \ \theta_0 = \frac{\alpha_1}{1+\alpha_1}e^{-\eta}, \ \phi_0 = \frac{\alpha_2}{1+\alpha_2}e^{-\eta}, \tag{17}$$

$$\mathcal{L}_f = f''' - f', \ \mathcal{L}_\theta = \theta'' - \theta, \ \mathcal{L}_\phi = \phi'' - \phi. \tag{18}$$

Such that,

$$\mathcal{L}_f^*\left[D_1 + D_2 e^{\eta} + D_3 e^{-\eta}\right] = 0, \ \mathcal{L}_\theta^*\left[D_4 e^{\eta} + D_5 e^{-\eta}\right] = 0, \ \mathcal{L}_\phi^*\left[D_6 e^{\eta} + D_7 e^{-\eta}\right] = 0, \tag{19}$$

where D_i $(i = 1-7)$ are calculated through BCs. 0th order problems, are defined as,

$$\mathcal{N}_f = (1+K)\frac{\partial^3 \tilde{f}}{\partial \eta^3} + \hat{f}\frac{\partial^2 \tilde{f}}{\partial \eta^2} - \left(\frac{\partial \tilde{f}}{\partial \eta}\right)^2 - K\Lambda\left(\frac{\partial^2 \tilde{f}}{\partial \eta^2}\right)^2 \frac{\partial^3 \tilde{f}}{\partial \eta^3} + Q\exp(-\beta\eta), \quad (20)$$

$$\mathcal{N}_\theta = \left(1+\frac{4}{3}Rd\right)\frac{\partial^2 \tilde{\theta}}{\partial \eta^2} + \Pr\left(Nb\frac{\partial \tilde{\phi}}{\partial \eta}\frac{\partial \tilde{\theta}}{\partial \eta} + \tilde{f}\frac{\partial \tilde{\theta}}{\partial \eta} + Nt\left(\frac{\partial \tilde{\theta}}{\partial \eta}\right)^2\right), \quad (21)$$

$$\mathcal{N}_\phi = \frac{\partial^2 \tilde{\phi}}{\partial \eta^2} + PrLe\left(\tilde{f}\frac{\partial \tilde{\phi}}{\partial \eta} - K_1\phi\right) + \frac{Nt}{Nb}\frac{\partial^2 \tilde{\theta}}{\partial \eta^2}. \quad (22)$$

Setting $p = 0, 1$,

$$\begin{aligned} &\tilde{f}(\eta,p) = f_0, \quad \tilde{\theta}(\eta,p) = \theta_0, \quad \tilde{\phi}(\eta,p) = \phi_0, \quad \text{at} \quad p = 0,\\ &\tilde{f}(\eta;p) = f, \quad \tilde{\theta}(\eta,p) = \theta, \quad \tilde{\phi}(\eta,p) = \phi, \quad \text{at} \quad p = 1. \end{aligned} \quad (23)$$

From initial guesses to final solutions, the value of p is varied from 0 to 1. Using Taylor's expansion and assuming that the expanded series converge for $p = 1$, the mth-order problems of deformation are defined below with subsequent boundary conditions,

$$\begin{aligned} \check{\mathcal{R}}_f^m(\eta) =& (1+K)f'''_{m-1} + \sum_{k=0}^{m-1} f_{m-1-k}\, f''_k - \sum_{k=0}^{m-1} f'_{m-1-k} \quad f'_k \\ &- K\Lambda\sum_{k=0}^{m-1} f''_{m-1-k}\sum_{l=0}^{k} f''_{k-l}f'''_l + Q\exp(-\beta\eta), \end{aligned} \quad (24)$$

$$\begin{aligned} \check{\mathcal{R}}_\theta^m(\eta) =& \left(1+\frac{4}{3}Rd\right)\theta''_{m-1} + \Pr\, Nb\sum_{k=0}^{m-1}\theta'_{m-1-k}\phi'_k + \Pr\sum_{k=0}^{m-1} f_{m-1-k}\theta'_k \\ &+ \Pr\, Nt\sum_{k=0}^{m-1}\theta'_{m-1-k}\theta'_k, \end{aligned} \quad (25)$$

$$\check{\mathcal{R}}_\phi^m(\eta) = \phi''_{m-1}(\eta) + \Pr\, Le\sum_{k=0}^{m-1} f_{m-1-k}\phi'_k - \Pr\, LeK_1\phi_{m-1}(\eta) + \frac{Nt}{Nb}\theta''_{m-1}, \quad (26)$$

$$\left.\begin{aligned} f_m(0) = 0, \quad f'_m(0) = 0, \quad \theta'_m(0) - \alpha_1\theta_m(0) = 0, \quad \phi'_m(0) - \alpha_2\phi_m(0) = 0,\\ f'_m(\infty) = 0, \quad \theta_m(\infty) = 0, \quad \phi_m(\infty) = 0, \end{aligned}\right\} \quad (27)$$

where, χ_m=1, for $m > 1$ and 0 otherwise. The general solutions are expressed below,

$$f_m(\eta) = f_m^*(\eta)CD_1 + D_2e^{\eta} + D_3e^{-\eta}, \quad (28)$$

$$\theta_m(\eta) = \theta_m^*(\eta) + D_4e^{\eta} + D_5e^{-\eta}, \quad (29)$$

$$\phi_m(\eta) = \phi_m^*(\eta) + D_6e^{\eta} + D_7e^{-\eta}, \quad (30)$$

where D_i $(i = 1-7)$ are found through BCs and asterisk is used for special solutions.

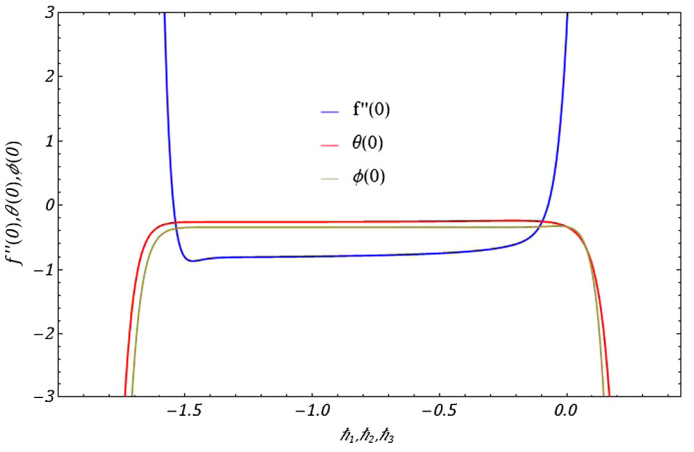

Figure 2. Convergence interval of f, θ and ϕ.

4. Analysis

The series solutions obtained through HAM involve auxiliary parameters. The parameters are called convergence controlling parameters and a speedy convergence is dependent on best choice of these parameters. The HAM-curves on the bases of suitable values for auxiliary parameters are plotted in Figure 2 for the three flow profiles velocity, temperature and concentration, respectively. The meaningful intervals of convergence for the three flow profiles are $[-1.5, -0.5]$, $[-1.5, 0.00]$ and $[-1.50, 0.00]$, respectively.

5. Results & discussion

In this section we explore the influence of various fluid parameters on the flow profiles. Fluid parameters like modified Hartman factor Q, dimensionless parameter β, fluid parameters K and Λ, the heat and mass Biot numbers α_1, α_2, Brownian motion factor Nb and Thermophoretic parameter Nt, radiation parameter Rd, Prandtl factor Pr, Lewis number Le and chemical reaction K_1 are of significant importance. Figures 3, 4 and 5 present the influence of β, K and Q on the velocity profile. The dimensionless parameter β significantly reduces the flow profile. The enhanced values of β continuously enhance the fluid viscosity that results in slow motion of the fluid and the profile declines. Figure 4 display the influence of K on velocity field and corresponding boundary layer. An enhancement in velocity is noticed towards augmented values of the respective fluid parameter. K is inverse of fluid viscosity μ. An enhancement in K results in reduction of viscosity of the fluid that ultimately, enhances the velocity profile. The modified Hartman factor Q results in enhancement in velocity field as displayed in Figure 5. The Lorentz forces generated by Riga plate parallel to the surface result in more surface tension. This tension, agitates the fluid to flow with enhanced velocity that results in augmenting

 https://doi.org/10.1016/j.heliyon.2019.e01479

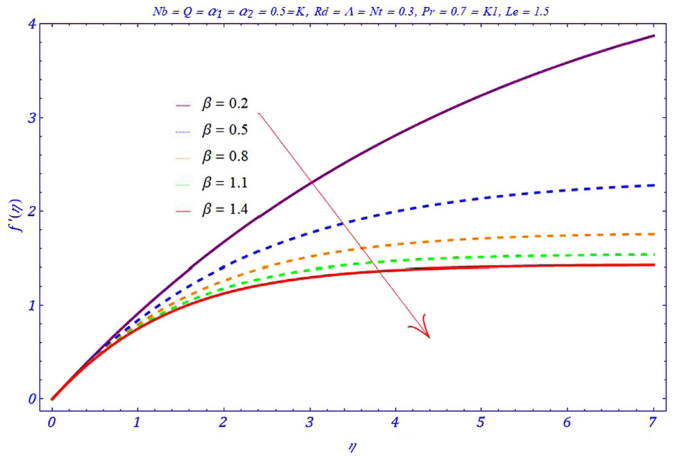

Figure 3. Impact of β on $f'(\eta)$.

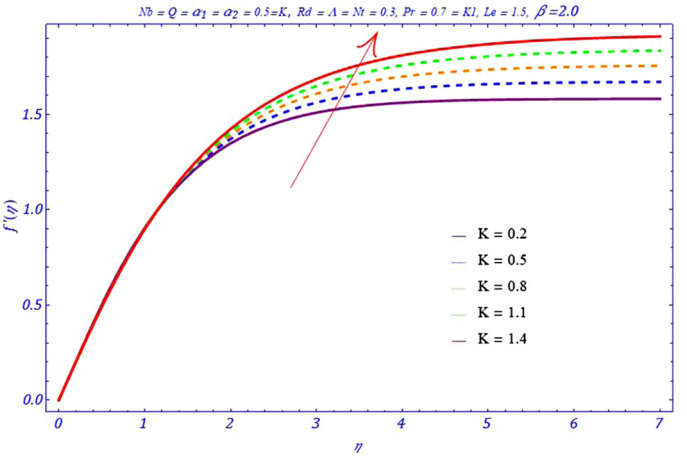

Figure 4. Impact of K on $f'(\eta)$.

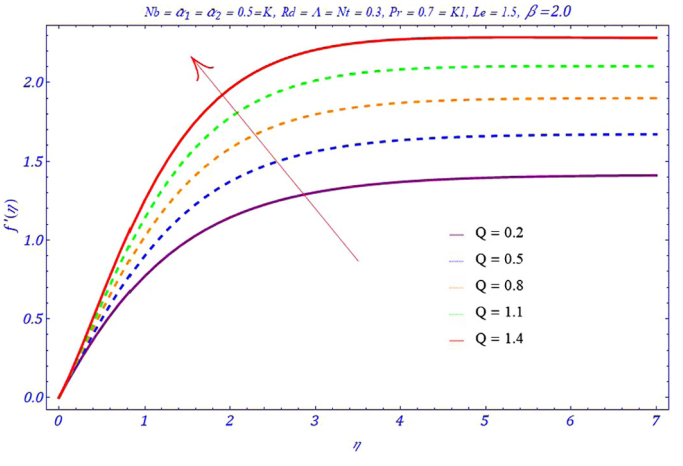

Figure 5. Impact of Q on $f'(\eta)$.

https://doi.org/10.1016/j.heliyon.2019.e01479

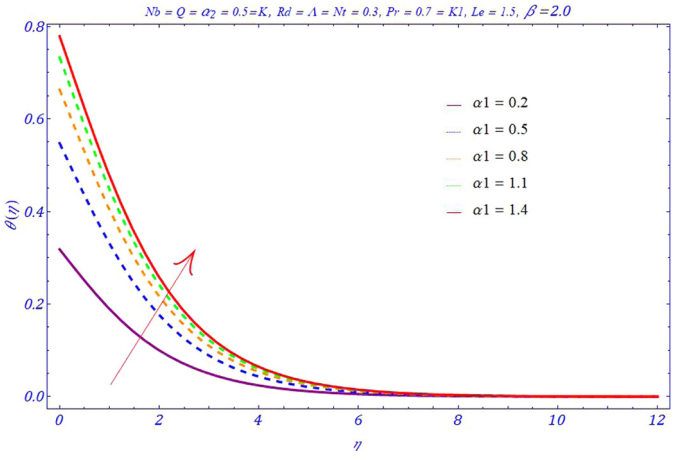

Figure 6. Impact of α_1 on $\theta(\eta)$.

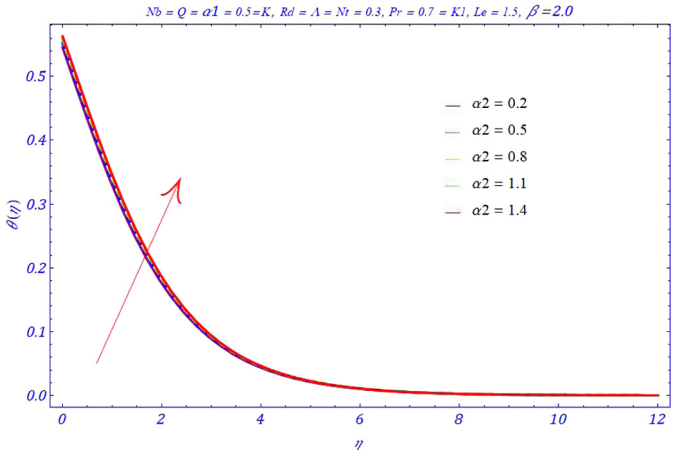

Figure 7. Impact of α_2 on $\theta(\eta)$.

the corresponding boundary layer. Figures 6, 7, 8, 9, 10, 11, 12 and 13 are the graphs of various fluid parameters on thermal profile. In particular, Figure 6 presents the influence of α_1 on temperature profile. Enhancement in α_1 results in a more stronger convection that rises the temperature profile. Consequently, the associated boundary layer augments for enhanced values of α_1. Figure 7 presents the influence of α_2 on the temperature profile. The enhanced α_2 results in increased mass convection. This enhancement results in rise of the temperature profile and corresponding boundary layer. An augment in K results in reduction of temperature and corresponding boundary layer as portrayed in Figure 8.

The dynamic viscosity involved in γ reduces with enhanced values of K that reduces the temperature profile. Both, the Brownian motion factor and Thermophoresis effect result in rise of the temperature profile as presented in Figure 9 and Figure 10. The un-predictive motion of fluid particles enhances with a stronger Brownian motion effect under the action of a strong Thermophoretic force generated by

 https://doi.org/10.1016/j.heliyon.2019.e01479

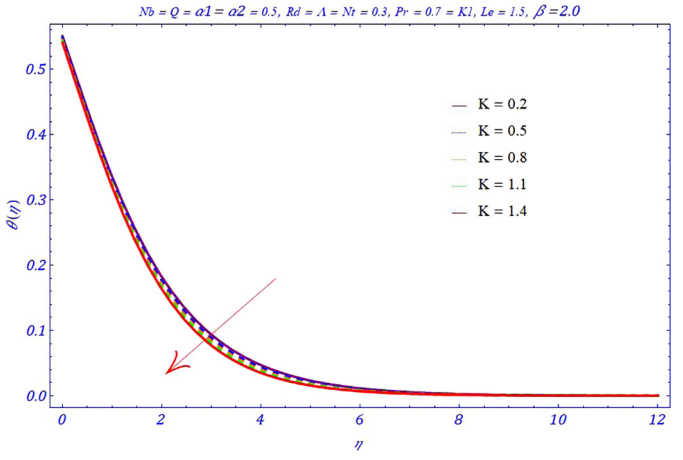

Figure 8. Impact of K on $\theta(\eta)$.

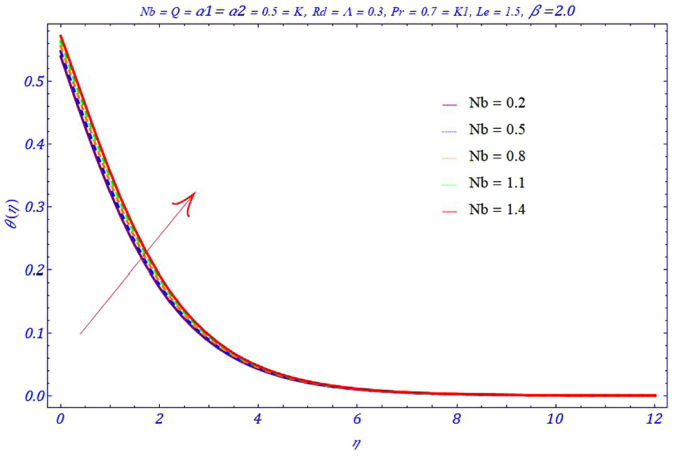

Figure 9. Impact of Nb on $\theta(\eta)$.

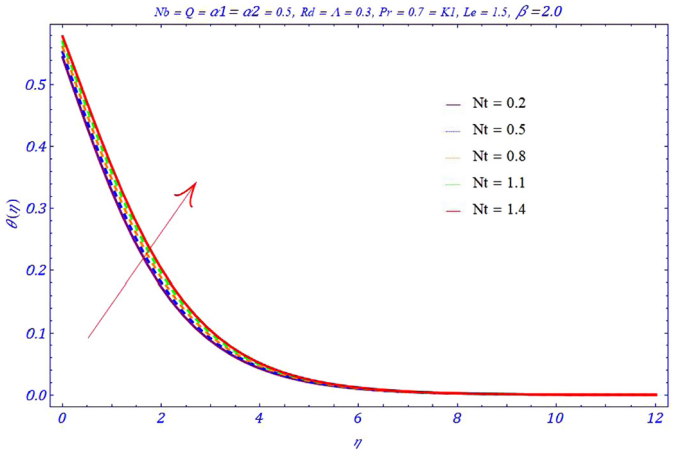

Figure 10. Impact of Nt on $\theta(\eta)$.

 https://doi.org/10.1016/j.heliyon.2019.e01479

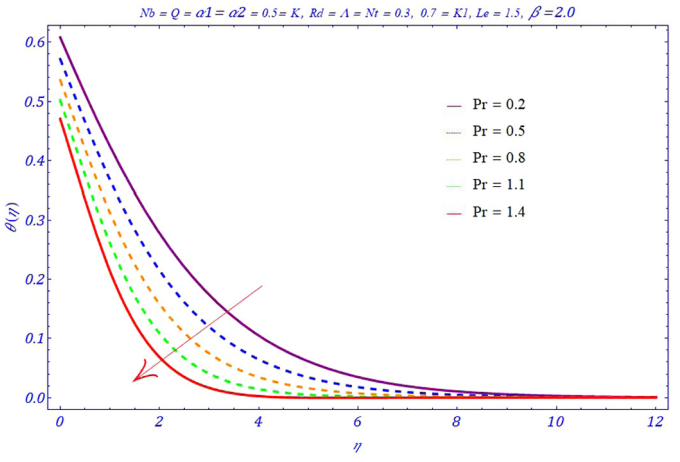

Figure 11. Impact of Pr on $\theta(\eta)$.

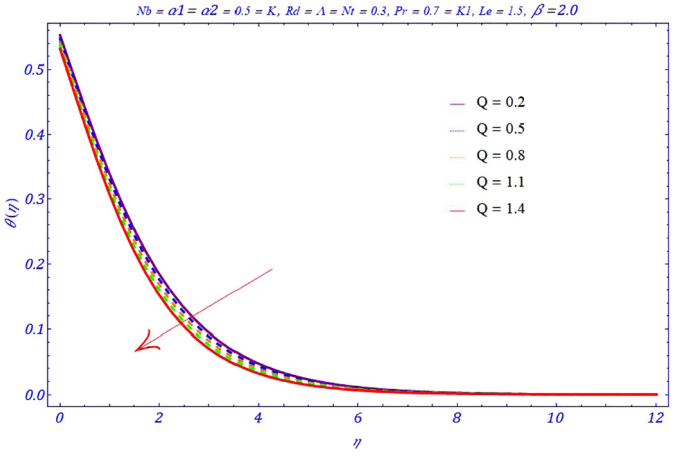

Figure 12. Impact of Q on $\theta(\eta)$.

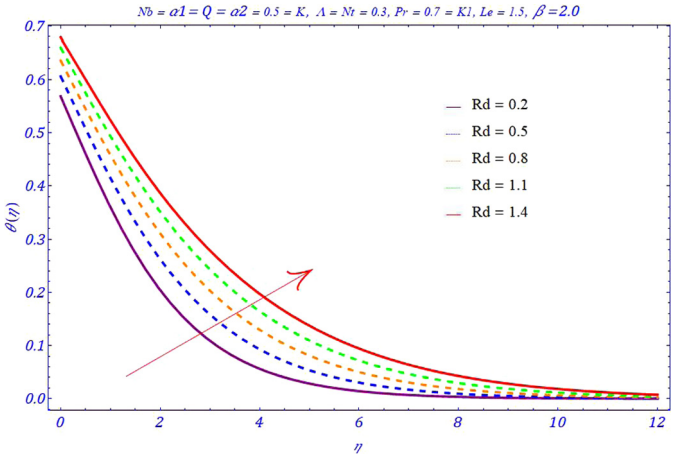

Figure 13. Impact of Rd on $\theta(\eta)$.

 https://doi.org/10.1016/j.heliyon.2019.e01479

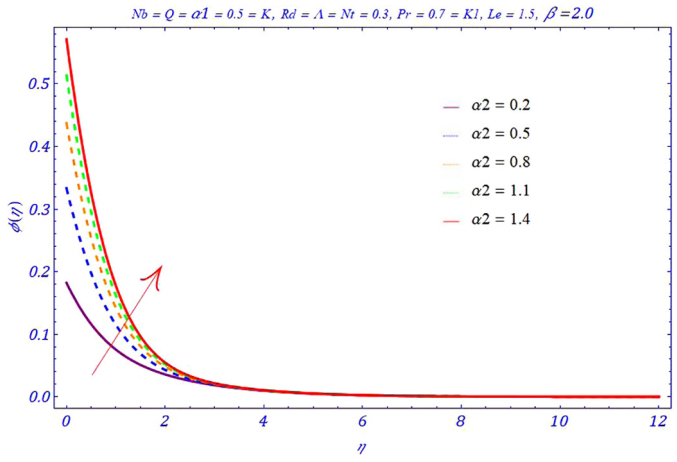

Figure 14. Impact of α_2 on $\phi(\eta)$.

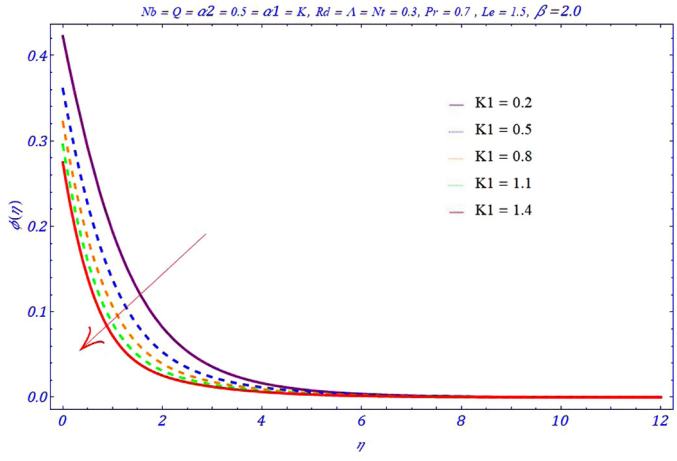

Figure 15. Impact of K_1 on $\phi(\eta)$.

the stronger Thermophoresis factor. Consequently, the temperature profile and associated boundary layer increase with augmented values of the Nb and Nt, respectively. The momentum to mass diffusivity ratio directly influence the temperature profile portrayed in Figure 11. A decreasing behavior is noticed towards augmented values of the involved parameter i.e. Pr. The stronger modified Hartman number results in decline of temperature profile and corresponding boundary layer as visualized in Figure 12. Figure 13 presents the effect of Radiation parameter on thermal profile. The enhanced values of radiation parameter result in enhancement of the temperature due to a stronger heat source. Figures 14, 15, 16 and 17 are the graphs of various parameters against the concentration profile. The enhanced α_2 results in enhancement of concentration as displayed in Figure 14. The Biot factor is related to the mass convection. The stronger mass Biot number results in higher concentration profile and enhanced thickness of boundary layer. Figure 15 is the impact of chemical reaction on the concentration profile. The enhanced values

 https://doi.org/10.1016/j.heliyon.2019.e01479

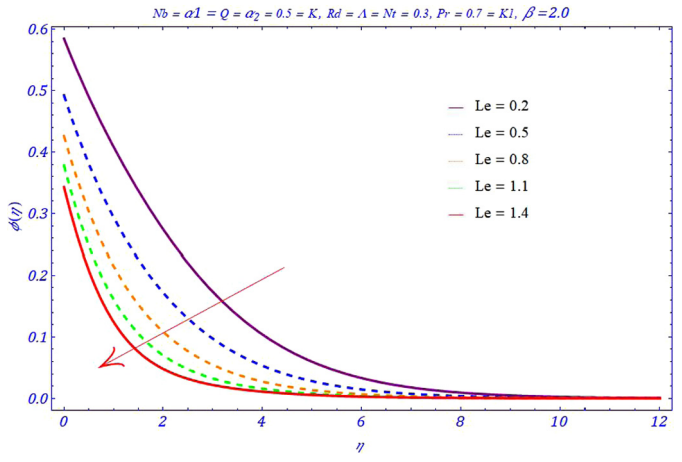

Figure 16. Impact of Le on $\phi(\eta)$.

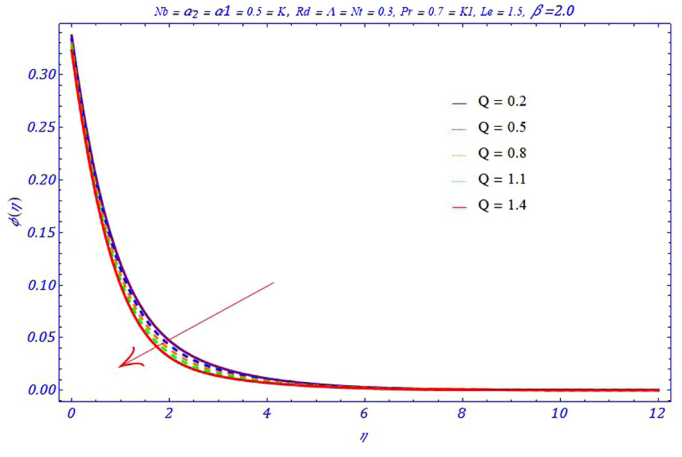

Figure 17. Impact of Q on $\phi(\eta)$.

of K_1 result in an enhanced penetration of fluid particles near the surface that reduces the associated boundary layer. Figures 16 and 17 are the graphs of Lewis number and modified Hartman numbers against concentration profile, respectively. The concentration profile is found as a decreasing function of both the parameters. Table 1 is compiled on the basis of data obtained through numerical simulation in Mathematica 9.0 using HAM based code. The results are presented to analyze the behavior of skin friction against pertinent parameters. The drag force (skin-friction) is found as an increasing function of β and K. However, the force reduces with augmented values of the modified Hartman number. Data presented in Table 2 is obtained for Nusselt and Sherwood numbers for various pertinent parameters. The values are varied from 0.0 to 1.0. Clearly, the heat flux enhances with augmented values of Q, Rd and K_1. It reduces with augmented values of β, Λ, Nb and Nt. The mass flux enhances with augmented values of Q, Nb, Rd and K_1.

Table 1. Numerical data of Skin-friction (Drag force) for various fluid parameters.

β	K	Q	$-\mathrm{Re}_x^{1/2} C_{fx}$
0.0	0.3	0.3	0.63628
0.5			0.79809
1.0			0.87679
2.0	0.0	0.3	0.39629
	0.5		0.50698
	1.0		0.61517
2.0	0.3	0.0	1.0920
		0.5	0.46026
		1.0	0.11377

Table 2. Numerical data of Nusselt number (heat flux) and Sherwood number (mass flux) for different values of fluid parameters.

β	Q	Λ	Nb	Nt	Rd	K_1	$\mathrm{Re}_x^{-1/2} Nu_x$	$\mathrm{Re}_x^{-1/2} Sh_x$
0.0	0.5	0.3	0.5	0.3	0.3	0.7	0.3459	0.3469
0.5							0.3305	0.3363
1.0							0.3252	0.3327
2.0	0.0	0.3	0.5	0.3	0.3	0.7	0.3181	0.3280
	0.5						0.3213	0.3301
	1.0						0.3245	0.3323
2.0	0.5	0.0	0.5	0.3	0.3	0.7	0.3214	0.3302
		0.5					0.3213	0.3301
		1.0					0.3211	0.3301
2.0	0.5	0.3	0.1	0.3	0.3	0.7	0.3286	0.2724
			0.6				0.3195	0.3326
			1.1				0.3104	0.3380
2.0	0.5	0.3	0.5	0.0	0.3	0.7	0.3269	0.3432
				0.5			0.3176	0.3222
				1.0			0.3084	0.3052
2.0	0.5	0.3	0.5	0.3	0.0	0.7	0.2509	0.3269
					0.5		0.3636	0.3317
					1.0		0.4608	0.3350
2.0	0.5	0.3	0.5	0.3	0.3	0.0	0.3210	0.2528
						0.5	0.3212	0.3154
						1.0	0.3216	0.3462

6. Conclusions

We considered an in-compressible Powell-Eyring nanofluid flow along a radiative Riga surface in two-dimensions. Convective conditions have been utilized along with the first order chemical reaction effect. Following are salient conclusions of this numerical study:

- The velocity field enhances for augmented values of modified Hartman number whereas a reduction is noticed in thermal and solutal boundary layers.
- The enhanced K_1 effect reduces the nanoparticles concentration near the radiative Riga surface.
- Enhancement in radiation effect enhances the thermal boundary layer.

https://doi.org/10.1016/j.heliyon.2019.e01479

- Temperature is decreasing function of Pr, Q and K.
- Both α_1 and α_2 are increasing factors for temperature profile. An enhancement is noticed in concentration profile with enhancement in mass Biot number.
- Brownian motion factor and Thermophoresis result in enhancement of thermal boundary layer.
- Concentration profile declines for stronger values of Lewis number.
- The wall drag force (skin-friction) is found a mounting function of β and K. However, the force reduces with augmented values of the Q.
- The heat flux enhances with augmented values of Q, Rd and K_1. It reduces with augmented values of Λ, Nb, β, and Nt.
- The mass flux enhances with augmented values of Nb, Rd, Q, and K_1.

Declarations

Author contribution statement

Ghulam Rasool: Conceived and designed the analysis; Analyzed and interpreted the data; Wrote the paper.

Ting Zhang: Contributed analysis tools or data.

Funding statement

This research did not receive any specific grant from funding agencies in the public, commercial, or not-for-profit sectors.

Competing interest statement

The authors declare no conflict of interest.

Additional information

No additional information is available for this paper.

References

[1] S.U.S. Choi, J.A. Eastman, Enhancing thermal conductivity of fluids with nanoparticles, in: Enhancing Thermal Conductivity of Fluids with Nanoparticles, 1995, pp. 99–105.

[2] J. Buongiorno, Convective transport in nanofluids, J. Heat Transf. 128 (2006) 240–250.

[3] A.V. Kuznetsov, D.A. Nield, The Cheng-Minkowycz problem for natural convective boundary layer flow in a porous medium saturated by a nanofluid: a revised model, Int. J. Heat Mass Transf. 65 (2013) 682–685.

[4] M. Sheikholeslami, M.G. Bandpy, R. Ellahi, M. Hassan, S. Soleimani, Effects of MHD on Cu-water nanofluid flow and heat transfer by means of CVFEM, J. Magn. Magn. Mater. 349 (2014) 188–200.

[5] M. Mustafa, T. Hayat, I. Pop, S. Asghar, S. Obaidat, Stagnation-point flow of a nanofluid towards a stretching sheet, Int. J. Heat Mass Transf. 54 (2011) 5588–5594.

[6] M. Turkyilmazoglu, Exact analytical solutions for heat and mass transfer of MHD slip flow in nanofluids, Chem. Eng. Sci. 84 (2012) 182–187.

[7] K.L. Hsiao, Nanofluid flow with multimedia physical features for conjugate mixed convection and radiation, Comput. Fluids 104 (2014) 1–8.

[8] A. Malvandi, D.D. Ganji, Brownian motion and thermophoresis effects on slip flow of alumina/water nanofluid inside a circular microchannel in the presence of a magnetic field, Int. J. Therm. Sci. 84 (2014) 196–206.

[9] C. Zhang, L. Zheng, X. Zhang, G. Chen, MHD flow and radiation heat transfer of nanofluids in porous media with variable surface heat flux and chemical reaction, Appl. Math. Model. 39 (2015) 165–181.

[10] M. Sheikholeslami, D.D. Ganji, M.Y. Javed, R. Ellahi, Effect of thermal radiation on magnetohydrodynamics nanofluid flow and heat transfer by means of two phase model, J. Magn. Magn. Mater. 374 (2015) 36–43.

[11] A. Malvandi, M.R. Safaei, M.H. Kaffash, D.D. Ganji, MHD mixed convection in a vertical annulus filled with Al_2O_3–water nanofluid considering nanoparticle migration, J. Magn. Magn. Mater. 382 (2015) 296–306.

[12] B.J. Gireesha, R.S.R. Gorla, B. Mahanthesh, Effect of suspended nanoparticles on three-dimensional MHD flow, heat and mass transfer of radiating Eyring-Powell fluid over a stretching sheet, J. Nanofluids 4 (2015) 474–484.

[13] T. Hayat, T. Muhammad, A. Alsaedi, M.S. Alhuthali, Magnetohydrodynamic threedimensional flow of viscoelastic nanofluid in the presence of nonlinear thermal radiation, J. Magn. Magn. Mater. 385 (2015) 222–229.

[14] T. Hayat, T. Muhammad, S.A. Shehzad, G.Q. Chen, I.A. Abbas, Interaction of magnetic field in flow of Maxwell nanofluid with convective effect, J. Magn. Magn. Mater. 389 (2015) 48–55.

 https://doi.org/10.1016/j.heliyon.2019.e01479

[15] A. Chamkha, S. Abbasbandy, A.M. Rashad, Non-Darcy natural convection flow for non-Newtonian nanofluid over cone saturated in porous medium with uniform heat and volume fraction fluxes, Int. J. Numer. Methods Heat Fluid Flow 25 (2015) 422–437.

[16] A. Zeeshan, A. Majeed, R. Ellahi, Effect of magnetic dipole on viscous ferrofluid past a stretching surface with thermal radiation, J. Mol. Liq. 215 (2016) 549–554.

[17] T. Mustafa, Buongiorno model in a nanofluid filled asymmetric channel fulfilling zero net particle flux at the walls, Int. J. Heat Mass Transf. 126 (2018) 974–979.

[18] M. Yuan, M. Rasul, M.M. Rashidi, Y. Zhigang, Study of nanofluid forced convection heat transfer in a bent channel by means of lattice Boltzmann method, Phys. Fluids 30 (3) (2018).

[19] N. Makulati, A. Kasaeipoor, M.M. Rashidi, Numerical study of natural convection of a water–alumina nanofluid in inclined C-shaped enclosures under the effect of magnetic field, Adv. Powder Technol. 27 (2) (2016) 661–672.

[20] M.M. Rashidi, M.M. Bhatti, M.A. Abbas, M.E. Ali, Entropy generation on MHD blood flow of nanofluid due to peristaltic waves, Entropy (18) (2016) 117.

[21] N. Freidoonimehr, B. Rostami, M.M. Rashidi, E. Momoniat, Analytical modelling of three-dimensional squeezing nanofluid flow in a rotating channel on a lower stretching porous wall, Math. Probl. Eng. (2014).

[22] A. Gailitis, O. Lielausis, On a possibility to reduce the hydrodynamic resistance of a plate in an electrolyte, Appl. Mag. Rep. Phys. Inst. 12 (1961) 143–146.

[23] R. Ahmad, M. Mustafa, M. Turkyilmazoglu, Buoyancy effects on nanofluid flow past a convectively heated vertical Riga-plate: a numerical study, Int. J. Heat Mass Transf. 111 (2017) 827–835.

[24] M. Sheikholeslami, A.J. Chamkha, Influence of Lorentz forces on nanofluid forced convection considering Marangoni convection, J. Mol. Liq. 225 (2017) 750–757.

[25] A. Shafiq, Z. Hammouch, A. Turab, Impact of radiation in a stagnation point flow of Walters' B fluid towards a Riga plate, Therm. Sci. Eng. Prog. 6 (2018) 27–33.

[26] A. Adeel, A. Saleem, A. Sumaira, Flow of nanofluid past a Riga plate, J. Magn. Magn. Mater. 402 (2016) 44–48.

[27] G. Rasool, T. Zhang, A. Shafiq, H. Durur, Influence of chemical reaction on Marangoni convective flow of nanofluid in the presence of Lorentz forces and thermal radiation: a numerical investigation, J. Adv. Nanotech. 1 (1) (2019) 32–49.

[28] M.A. Chaudhary, J.H. Merkin, A simple isothermal model for Homogeneous-heterogeneous reactions in boundary layer flow: II. Different diffusivities for reactant and autocatalyst, Fluid Dyn. Res. 16 (1995) 335–359.

[29] J.H. Merkin, A model for isothermal Homogeneous-heterogeneous reactions in boundary layer flow, Math. Comput. Model. 24 (1996) 125–136.

[30] M.A. Chaudhary, J.H. Merkin, Homogeneous-heterogeneous reactions in boundary-layer flow: effects of loss of reactant, Math. Comput. Model. 24 (1996) 21–28.

[31] W.A. Khan, I. Pop, Flow near the two-dimensional stagnation point on a infinite permeable wall with a homogeneous-heterogeneous reaction, Commun. Nonlinear Sci. Numer. Simul. 15 (2010) 3435–3443.

[32] W.A. Khan, I. Pop, Effect of homogeneous-heterogeneous reactions on the visco-elastic fluid towards a stretching sheet, J. Heat Transf. 134 (2012) 064506.

[33] R.E. Powell, H. Eyring, Mechanism for relaxation theory of viscosity, Nature 154 (1944) 427–428.

[34] M. Jalil, S. Asghar, S.M. Imran, Self similar solutions for the flow and heat transfer of Powell-Eyring fluid over a moving surface in a parallel free stream, Int. J. Heat Mass Transf. 65 (2013) 73–79.

[35] A. Mushtaq, M. Mustafa, T. Hayat, M. Rahi, A. Alsaedi, Exponentially stretching sheet in a Powell-Eyring fluid: numerical and series solutions, Z. Naturforsch. A 68a (2013) 791–798.

[36] M. Poonia, R. Bhargava, Finite element study of Eyring-Powell fluid flow with convective boundary conditions, J. Thermophys. Heat Transf. 28 (2014) 499–506.

[37] T. Hayat, S. Asad, M. Mustafa, A. Alsaedi, Radiation effects on the flow of Powell-Eyring fluid past an unsteady inclined stretching sheet with non-uniform heat source/sink, PLoS ONE 9 (2014) e103214.

[38] T. Hayat, M. Imtiaz, A. Alsaedi, Effects of homogeneous-heterogeneous reactions in flow of Powell-Eyring fluid, J. Cent. South Univ. 22 (2015) 3211–3216.

[39] T. Hayat, S. Hussain, T. Muhammad, A. Alsaedi, M. Ayub, Radiative flow of Powell-Eyring nanofluid with convective boundary conditions, Chin. J. Phys. 55 (4) (2017) 1523–1538.

[40] S.J. Liao, Homotopy analysis method: a new analytic method for nonlinear problems, Appl. Math. Mech. 19 (1998) 957.

[41] A. Shafiq, M. Nawaz, T. Hayat, A. Alsaedi, Magnetohydrodynamic axisymmetric flow of a third-grade fluid between two porous disks, Braz. J. Chem. Eng. 3 (2013) 599–609.

[42] A. Shafiq, S. Jabeen, T. Hayat, A. Alsaedi, Cattaneo-Christov heat flux model for squeezed flow of third grade fluid, Surf. Rev. Lett. 24 (2017) 1–11.

[43] A. Shafiq, Z. Hammouch, T.N. Sindhu, Bioconvective MHD flow of tangent hyperbolic nano-fluid with Newtonian heating, Int. J. Mech. Sci. 133 (2017) 759–766.

[44] A. Shafiq, T.N. Sindhu, Statistical study of hydromagnetic boundary layer flow of Williamson fluid regarding a radiative surface, Results Phys. 7 (2017) 3059–3067.

[45] R. Malik, M. Khan, A. Shafiq, M. Mushtaq, M. Hussain, An analysis of Cattaneo-Christov double-diffusion model for Sisko fluid flow with velocity slip, Results Phys. 7 (2017) 1232–1237.